



# X線バーストにおける重要不安定核 反応の実験的検証



## Experimental investigation of relevant unstable-nucleus reactions in X-ray bursts

Hidetoshi Yamaguchi  
山口英斉

*Center for Nuclear Study (CNS),  
the University of Tokyo*

# Topics

- Experimental evaluation of **reactions from an unstable nucleus (RI) to another RI** relevant for X-ray bursts  $\Rightarrow$  still challenging, due to the limited intensity of RI beams.

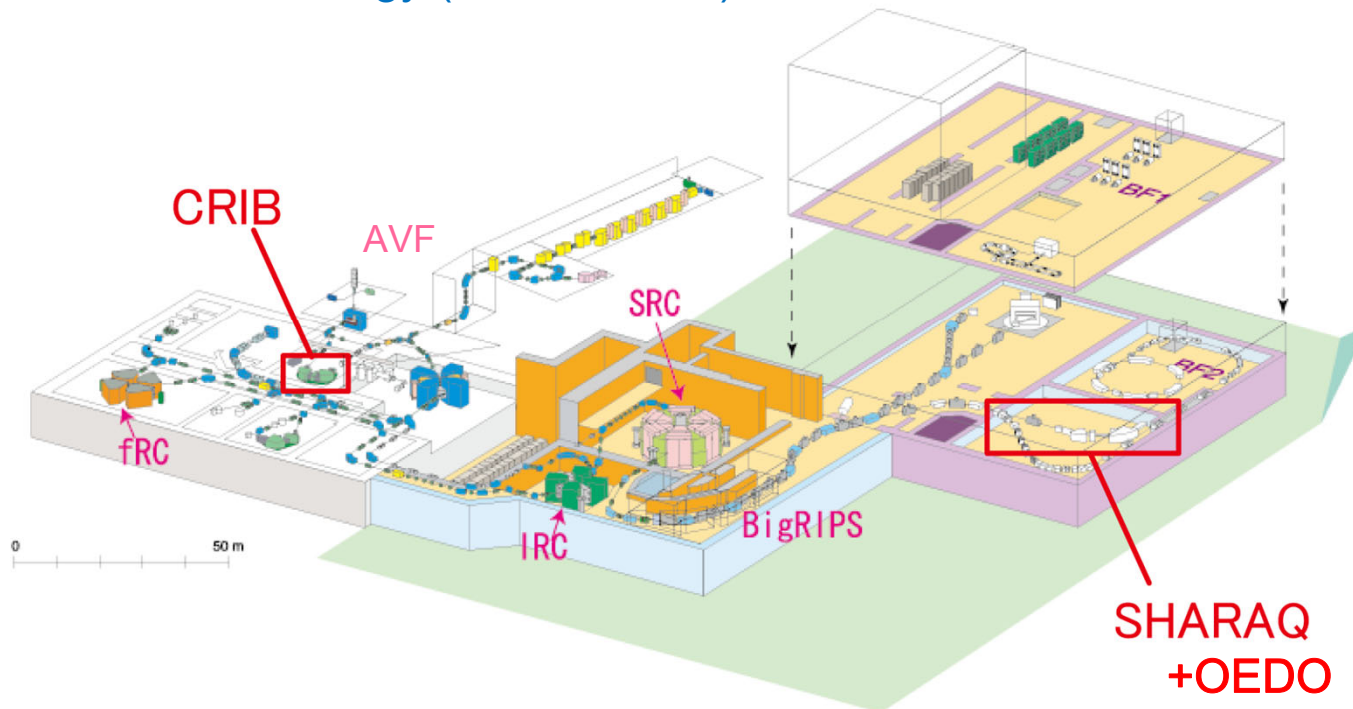
Two recent examples at CRIB (RI beam separator of U-Tokyo):

- ◆  $^{22}\text{Mg}(\alpha, p)^{25}\text{Al}$  reaction study with resonant scattering  
Jun Hu, H. Yamaguchi et al., *Phys. Rev. Lett.* **127**, 172701 (2021).
- ◆  $^{26}\text{Si}(\alpha, p)^{29}\text{P}$  reaction study with direct measurement  
Measurement performed in 2022, analysis in progress (K. Okawa's Ms thesis)

# CRIB/OEDO in RIBF

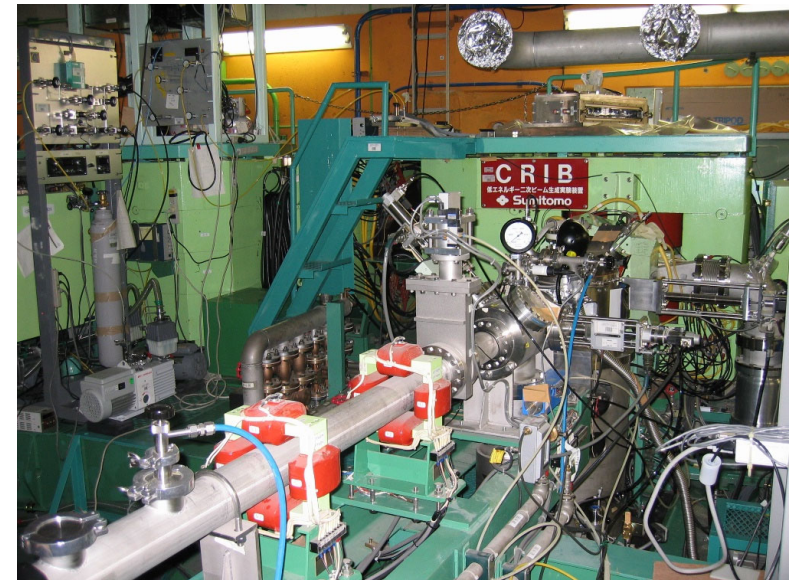
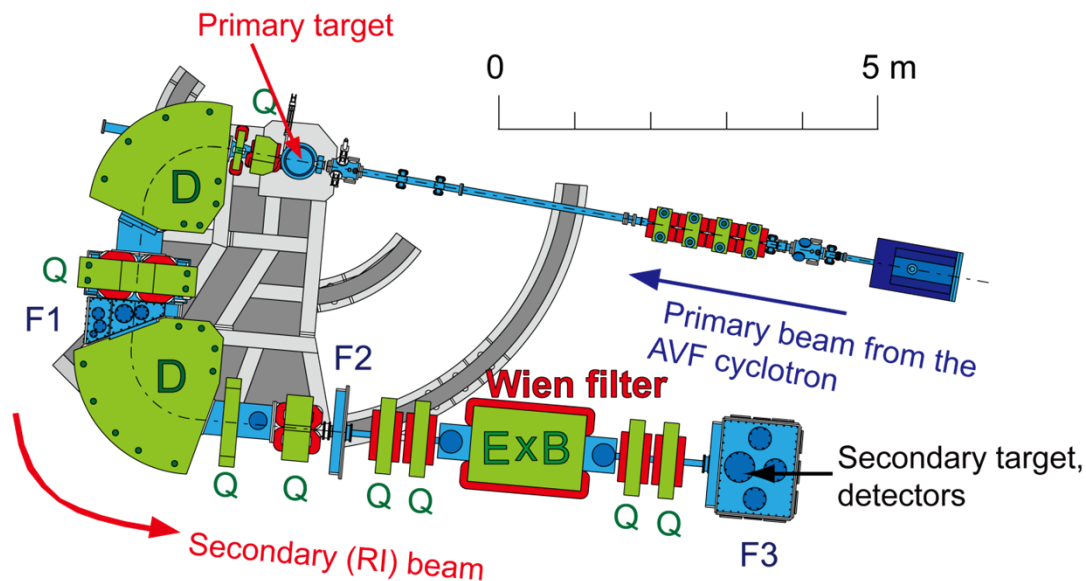
RI-beam apparatuses operated by CNS, the University of Tokyo at RIBF

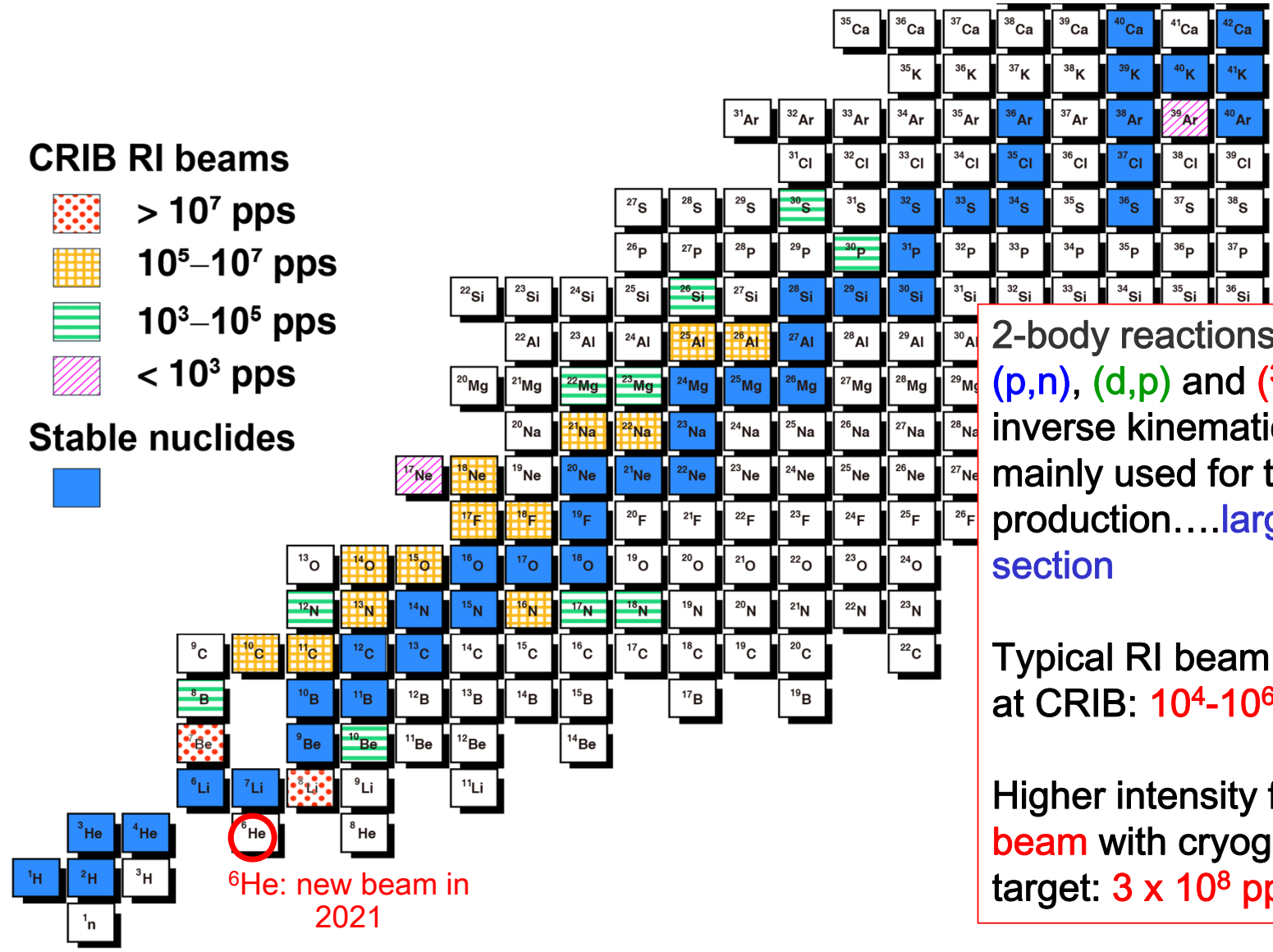
- CRIB: RI beam separator for low-mass, low-energy ( $<10$  MeV/u) RI beams
- SHARAQ: high resolution spectrometer
- OEDO: new low-energy (20-50 MeV/u) beamline for exotic beams



# CRIB – Low energy RI beam separator of CNS

- **CNS Radio-Isotope Beam separator**, operated by **CNS** (Univ. of Tokyo), located at **RIBF** (RIKEN Nishina Center).
  - ◆ **Low-energy (<10 MeV/u) RI beams** by in-flight method.
  - ◆ Primary beam from K=70 AVF cyclotron.
  - ◆ Momentum (Magnetic rigidity) separation by “double achromatic” system, and velocity separation by a Wien filter.





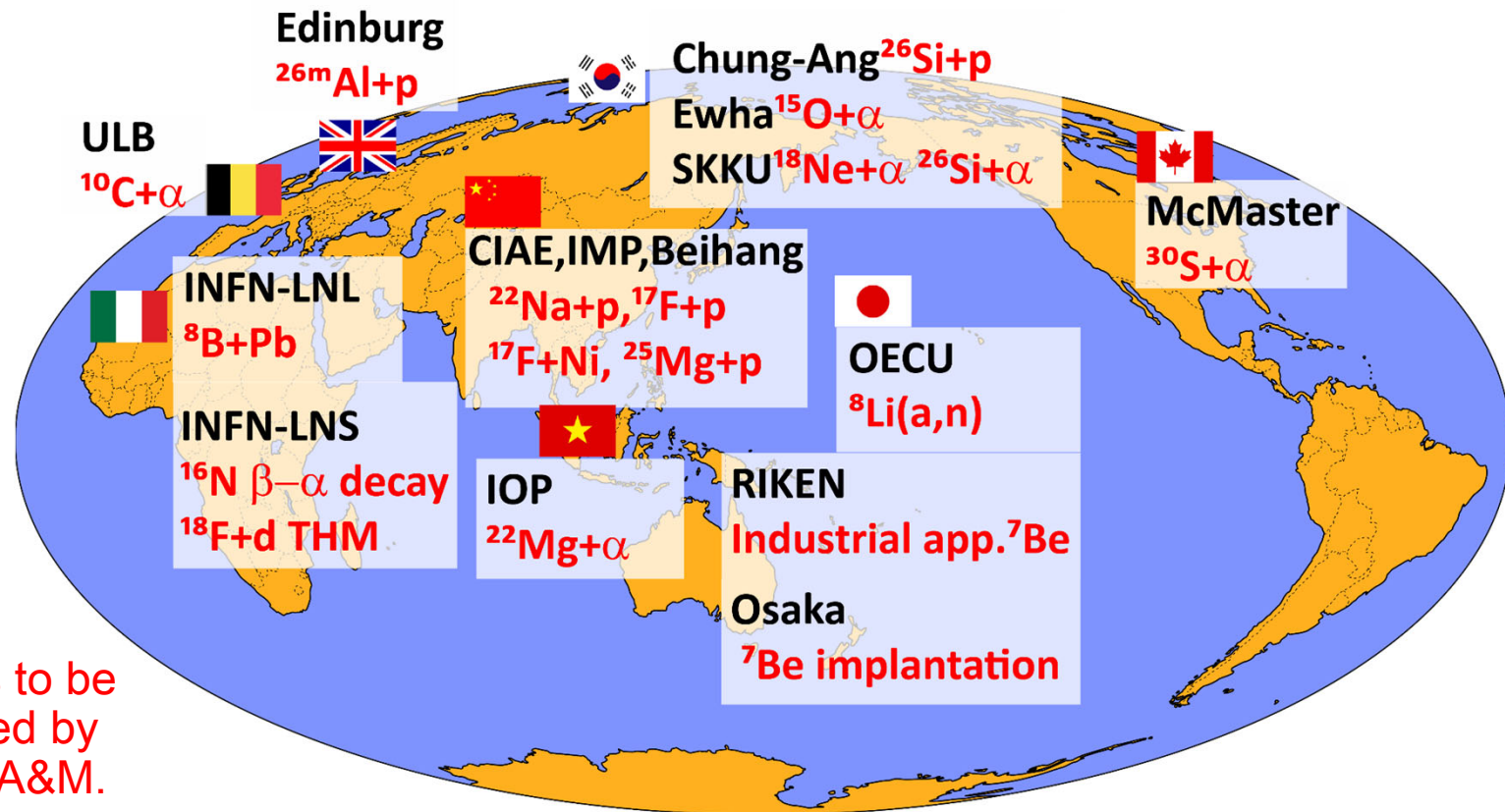
2-body reactions such as  $(p,n)$ ,  $(d,p)$  and  $({}^3\text{He},n)$  in inverse kinematics are mainly used for the production....large cross section

Typical RI beam intensity: at CRIB:  $10^4 - 10^6$  pps

Higher intensity for  ${}^7\text{Be}$  beam with cryogenic  $\text{H}_2$  target:  $3 \times 10^8$  pps.

# CRIB is collaborative

- Recent CRIB collaborators (only the main institutes that proposed an experiment are shown):

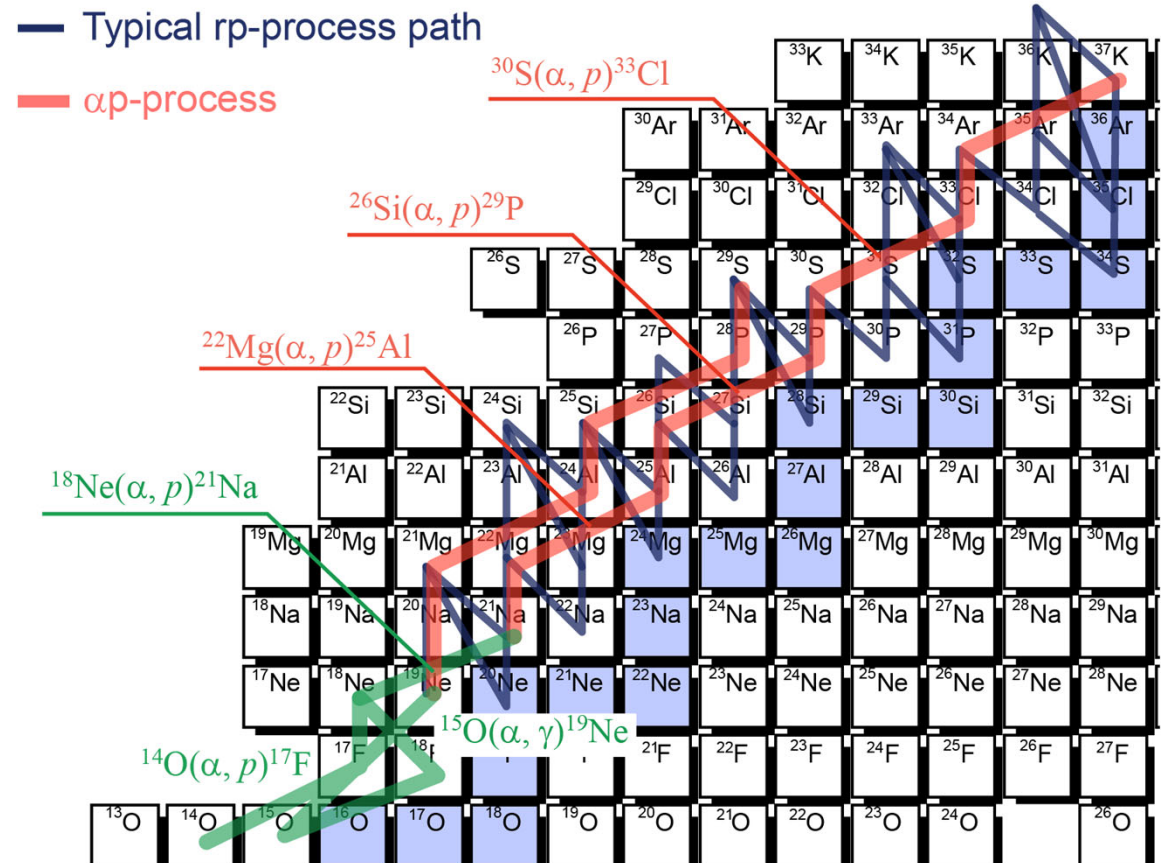


2023 Mar:

$^{14}\text{O}+\alpha$  experiment is to be performed, proposed by IBS(Korea)+Texas A&M.

# Key $\alpha$ -induced reactions in X-ray bursts

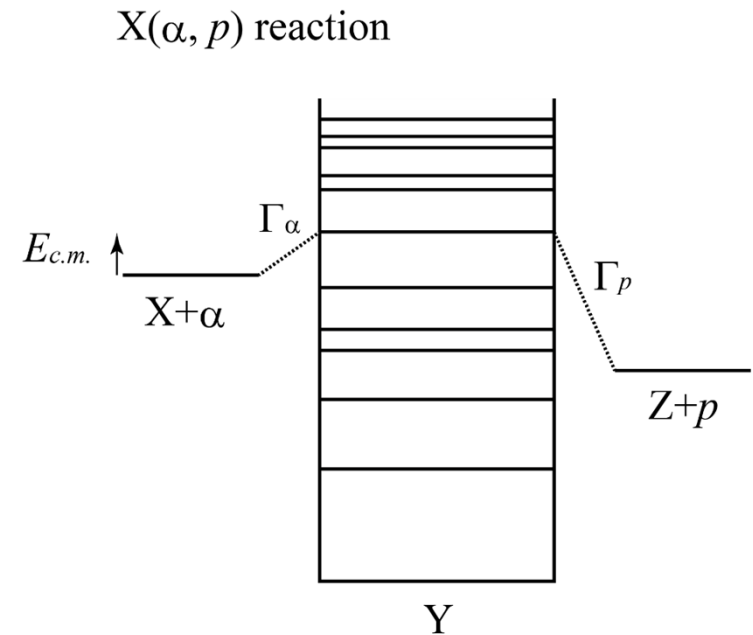
- The “rp-process” in X-ray bursts ( $T_{\max}$  can be 2-3 GK) takes a path including  $(\alpha, p)$  reactions to skip sequential  $(p, \gamma)$  and  $\beta$  decays... the  $\alpha p$ -process.
- Several key  $(\alpha, \gamma)$  and  $(\alpha, p)$  reactions, from an RI to another RI (i.e. difficult to study it experimentally) affect much to the X-ray light curve.



# Typical situation

For those **RI-to-RI astrophysical ( $\alpha, p$ ) reactions**,

- Reaction rates are often dominated by **resonant reactions**.
- Most effective reactions are **exothermic (positive Q-value)**. The  $p$  channel is located below the  $\alpha$  channel and  $\Gamma_\alpha \ll \Gamma_p$
- **Resonances just above the  $\alpha$  threshold** are most relevant;  $E_{c.m.}$  is small in stellar reactions,  $\sim 1$  MeV order at  $T=1$  GK.



# Study of resonance parameters

The Breit-Wigner formula:

$$\sigma(E) = \pi \tilde{\lambda}^2 \frac{2J+1}{(2J_1+1)(2J_2+1)} (1 + \delta_{12}) \frac{\Gamma_a \Gamma_b}{(E - E_0)^2 + (\Gamma/2)^2}$$

$\tilde{\lambda}$  : de Broglie wavelength

$J_1, J_2, J$  : spins of projectile, target, excited state in the compound nucleus

$\delta_{12}$  : 1 for identical particles, 0 otherwise

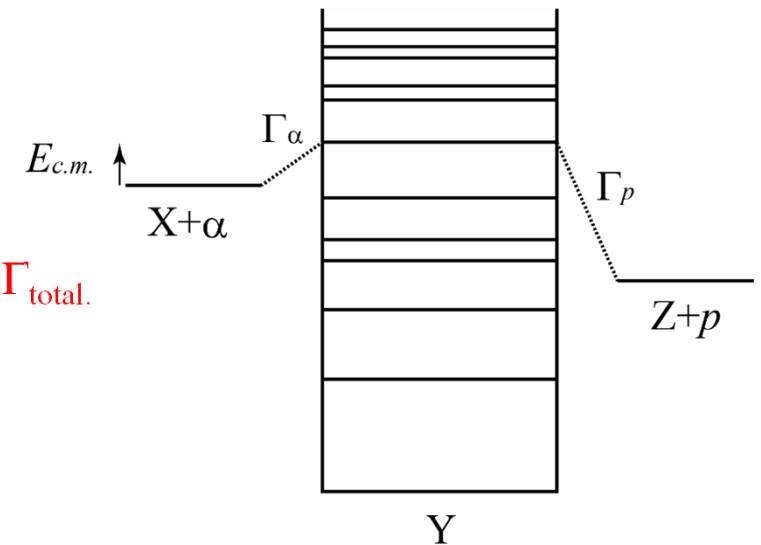
$\Gamma_a, \Gamma_b$  : Widths of entrance and exit channels

is telling us the resonant reaction cross section  $\sigma$  is known

by the resonance parameters:  $E_r, J^\pi$ , decay widths  $\Gamma_\alpha, \Gamma_p$ , and  $\Gamma_{\text{total}}$ .

- In the typical case,  $\Gamma_\alpha \ll \Gamma_p \sim \Gamma_{\text{total}}$   
this implies the effect of  $\Gamma_\alpha$  is greater than  $\Gamma_p$ .

$X(\alpha, p)$  reaction



# Resonant scattering from inverse reaction channel

- **Resonant scattering**...A good method to observe resonances with a high cross section (even feasible with RI beams). Resonance parameters can be determined by **R-matrix** analysis.

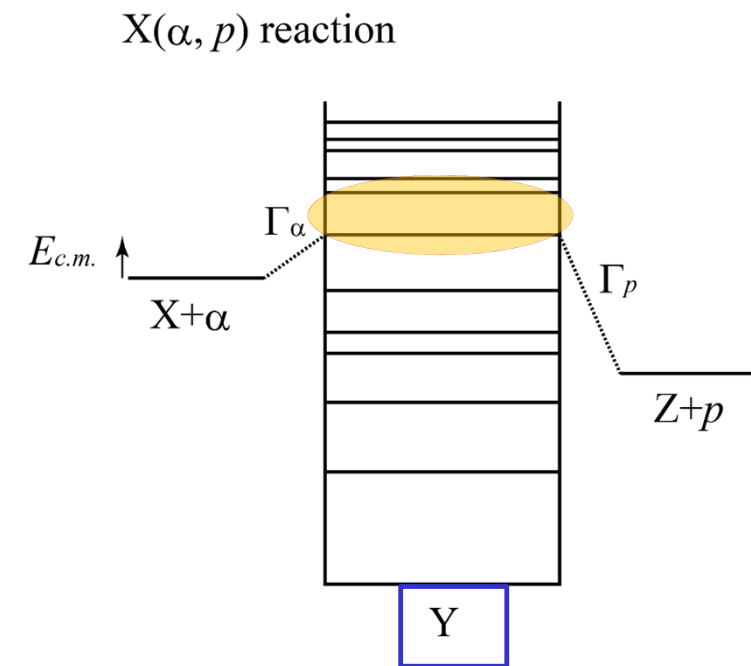
We can study **resonances** in **Y** via

**X+ $\alpha$**  scattering ( $\alpha$ -resonant scattering)

or inversely,

**Z+p** scattering (proton resonant scattering)

- **X+ $\alpha$** ...the scanned energy is quite low. The most relevant resonances (at Gamow energy) are buried under Rutherford scattering and **hardly seen**.
- **Z+p**...Thanks to the lower threshold energy, we can observe relevant resonances, and determine  $E_r$ ,  $J^\pi$ , and  $\Gamma_p$ , (but no  $\Gamma_\alpha$ ). “**Resonant scattering from inverse reaction channel**”.



# Our recent publication on $^{22}\text{Mg}(\alpha, p)$ : One application of the “resonant scattering from inverse reaction channel”



PHYSICAL REVIEW LETTERS **127**, 172701 (2021)

## Advancement of Photospheric Radius Expansion and Clocked Type-I X-Ray Burst Models with the New $^{22}\text{Mg}(\alpha, p)^{25}\text{Al}$ Reaction Rate Determined at the Gamow Energy

J. Hu (胡钧)<sup>1,2,\*</sup>, H. Yamaguchi (山口英齐)<sup>3,4</sup>, Y. H. Lam (藍乙華)<sup>1,2,†</sup>, A. Heger<sup>5,6,7,8</sup>, D. Kahl<sup>9,10</sup>, A. M. Jacobs,<sup>8,11</sup> Z. Johnston<sup>8,11</sup>, S. W. Xu (许世伟)<sup>1</sup>, N. T. Zhang (张宁涛)<sup>1</sup>, S. B. Ma (马少波)<sup>1</sup>, L. H. Ru (茹龙辉)<sup>1</sup>, E. Q. Liu (刘恩强)<sup>1</sup>, T. Liu (刘通)<sup>1</sup>, S. Hayakawa (早川勢也)<sup>3</sup>, L. Yang (杨磊)<sup>3,‡</sup>, H. Shimizu (清水英樹)<sup>3</sup>, C. B. Hamill,<sup>10</sup> A. St. J. Murphy,<sup>10</sup> J. Su (苏俊)<sup>12</sup>, X. Fang (方晓)<sup>13</sup>, K. Y. Chae (채경욱)<sup>14</sup>, M. S. Kwag (곽민식)<sup>14</sup>, S. M. Cha (차수미)<sup>14</sup>, N. N. Duy<sup>14,15</sup>, N. K. Uyen,<sup>14</sup> D. H. Kim (김두현)<sup>14</sup>, R. G. Pizzone<sup>16</sup>, M. La Cognata<sup>16</sup>, S. Cherubini,<sup>16</sup> S. Romano<sup>16,17,18</sup>, A. Tumino,<sup>16,19</sup> J. Liang,<sup>20</sup> A. Psaltis,<sup>20</sup> M. Sferrazza,<sup>21</sup> D. Kim (김다희),<sup>22</sup> Y. Y. Li (李依阳),<sup>1,2</sup> and S. Kubono (久保野茂)<sup>3,23</sup>

<sup>1</sup>Institute of Modern Physics, Chinese Academy of Sciences, Lanzhou 730000, China

<sup>2</sup>School of Nuclear Science and Technology, University of Chinese Academy of Sciences, Beijing 100049, China

<sup>3</sup>Center for Nuclear Study(CNS), the University of Tokyo, RIKEN campus, 2-1 Hirosawa, Wako, Saitama 351-0198, Japan

<sup>4</sup>National Astronomical Observatory of Japan, 2-21-1 Osawa, Mitaka, Tokyo 181-8588, Japan

<sup>5</sup>School of Physics and Astronomy, Monash University, Victoria 3800, Australia

<sup>6</sup>OzGrav-Monash—Monash Centre for Astrophysics, School of Physics and Astronomy, Monash University, Vic 3800, Australia

<sup>7</sup>Center of Excellence for Astrophysics in Three Dimensions (ASTRO-3D), Australia

<sup>8</sup>The Joint Institute for Nuclear Astrophysics, Michigan State University, East Lansing, Michigan 48824, USA

<sup>9</sup>Extreme Light Infrastructure - Nuclear Physics, IFIN-HH, 077125 Bucharest-Măgurele, Romania

<sup>10</sup>SUPA, School of Physics & Astronomy, University of Edinburgh, Edinburgh EH9 3FD, United Kingdom

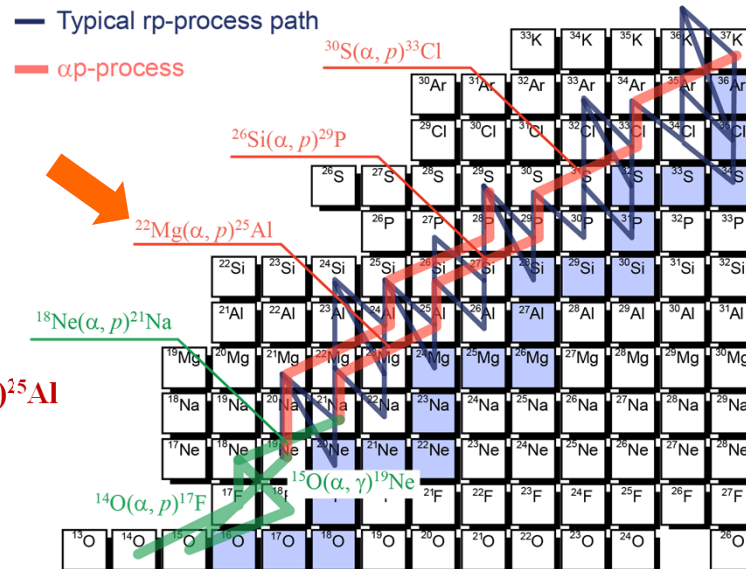
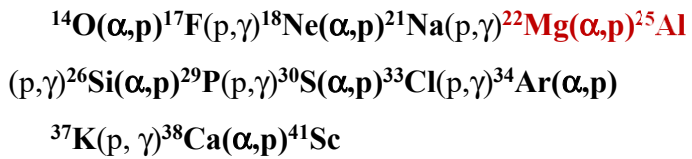
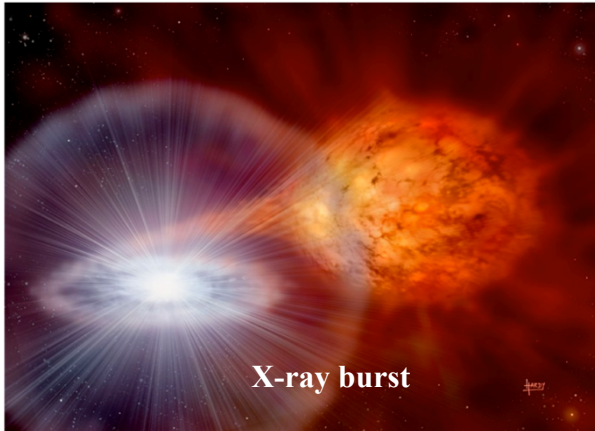
<sup>11</sup>Department of Physics and Astronomy, Michigan State University, East Lansing, Michigan 48824, USA

<sup>12</sup>Center of Modern Physics, Beijing Normal University, Beijing 100875, China



THE UNIVERSITY OF TOKYO

# $^{22}\text{Mg}(\alpha, p)$ in Type I X-ray bursts



R. Cyburt et al.

THE ASTROPHYSICAL JOURNAL, 830:55 (20pp), 2016 October 20

**Table 2**  
Reactions that Impact the Burst Light Curve  
in the Multi-zone X-ray Burst Model

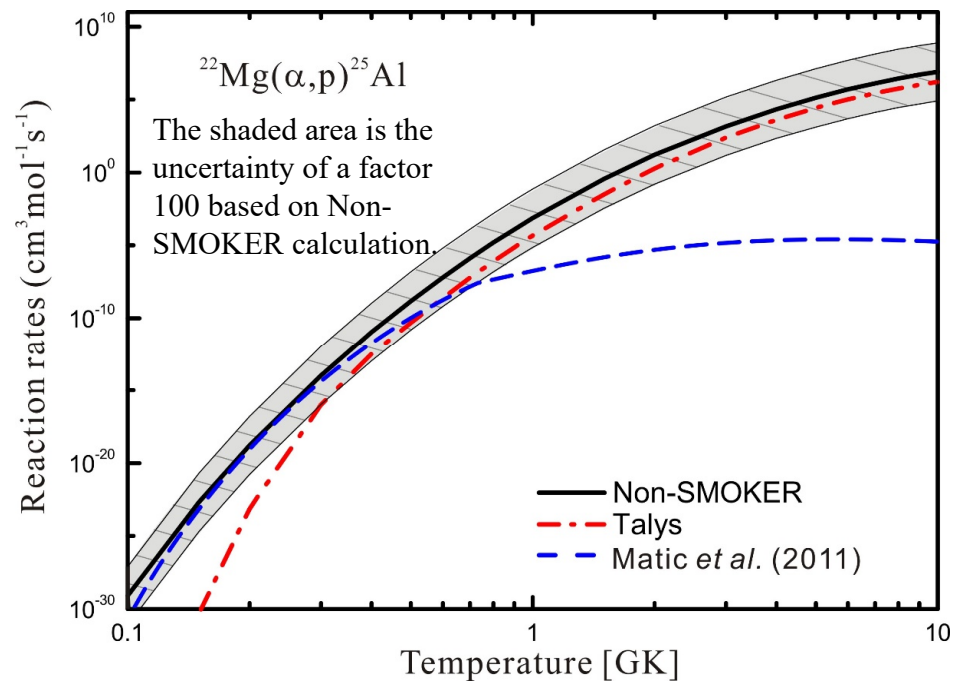
Rank	Reaction	Type <sup>a</sup>	Sensitivity <sup>b</sup>	Category
1	$^{15}\text{O}(\alpha, \gamma)^{19}\text{Ne}$	D	16	1
2	$^{56}\text{Ni}(\alpha, p)^{59}\text{Cu}$	U	6.4	1
3	$^{59}\text{Cu}(p, \gamma)^{60}\text{Zn}$	D	5.1	1
4	$^{61}\text{Ga}(p, \gamma)^{62}\text{Ge}$	D	3.7	1
5	$^{22}\text{Mg}(\alpha, p)^{25}\text{Al}$	D	2.3	1
6	$^{14}\text{O}(\alpha, p)^{17}\text{F}$	D	5.8	1
7	$^{23}\text{Al}(p, \gamma)^{24}\text{Si}$	D	4.6	1
8	$^{18}\text{Ne}(\alpha, p)^{21}\text{Na}$	U	1.8	1
9	$^{63}\text{Ga}(p, \gamma)^{64}\text{Ge}$	D	1.4	2
10	$^{19}\text{F}(p, \alpha)^{16}\text{O}$	U	1.3	2
11	$^{12}\text{C}(\alpha, \gamma)^{16}\text{O}$	U	2.1	2
12	$^{26}\text{Si}(\alpha, p)^{29}\text{P}$	U	1.8	2
13	$^{17}\text{F}(\alpha, p)^{20}\text{Ne}$	U	3.5	2
14	$^{24}\text{Mg}(\alpha, \gamma)^{28}\text{Si}$	U	1.2	2
15	$^{57}\text{Cu}(p, \gamma)^{58}\text{Zn}$	D	1.3	2
16	$^{60}\text{Zn}(\alpha, p)^{63}\text{Ga}$	U	1.1	2
17	$^{17}\text{F}(p, \gamma)^{18}\text{Ne}$	U	1.7	2
18	$^{40}\text{Sc}(p, \gamma)^{41}\text{Ti}$	D	1.1	2
19	$^{48}\text{Cr}(p, \gamma)^{49}\text{Mn}$	D	1.2	2

**Notes.**

<sup>a</sup> Up (U) or down (D) variation that has the largest impact.

<sup>b</sup>  $M_{IC}^{(i)}$  in units of  $10^{38} \text{ erg s}^{-1}$ .

## Status of $^{22}\text{Mg}(\alpha,p)^{25}\text{Al}$ astrophysical reaction rate evaluation (as of 2018)



Large difference between the experimental and theoretical calculations.

The  $^{22}\text{Mg}(\alpha,p)^{25}\text{Al}$  reaction rate as a function of the temperature for the Hauser-Feshbach predictions TALYS and non-SMOKER

# Direct measurement of $^{22}\text{Mg}(\alpha, p)$ at MSU

Randhawa et al., Phys. Rev. Lett (2020):  
First direct measurement of  $^{22}\text{Mg}(\alpha, p)$ .

NSCL;  $\sim 5$  MeV/u (broad?)  $^{22}\text{Mg}$  beam 900 cps,  
reaction measured with AT-TPC.

Data points only at energies corresponding to  $T >$   
2.6 GK (cf. most relevant  $T$  range they claim:  
below 1 GK).

Reaction rate evaluated by extrapolation down to  
the stellar energy with a statistical-model (NON-  
SMOKER) calculation. Reliable?

PHYSICAL REVIEW LETTERS 125, 202701 (2020)

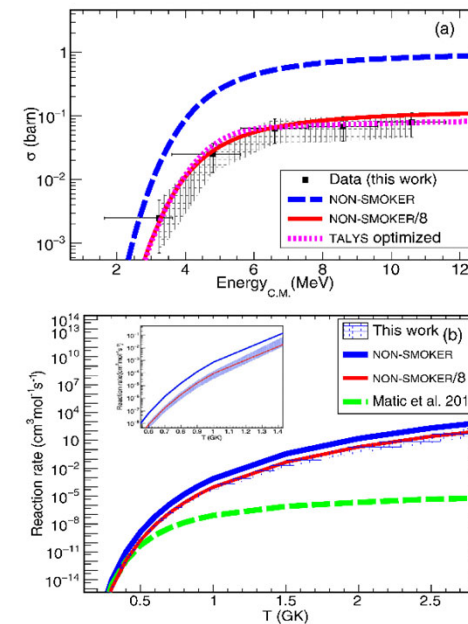
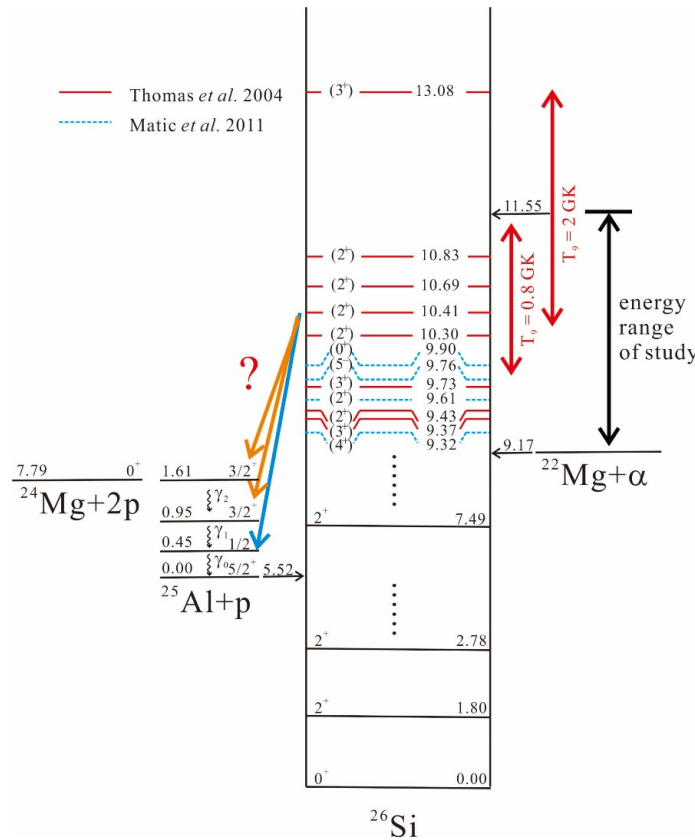


FIG. 3. Panel (a) shows the experimental cross sections obtained in the present work over a range of center-of-mass energies covered (black). For all the points, the cross section weighted energy is shown, which is the reason why horizontal error bars for the two lowest energy points are asymmetric. Panel (b) shows the reaction rate comparison of the current work to different model predictions and to the previous measurement by Matic *et al.* [11].

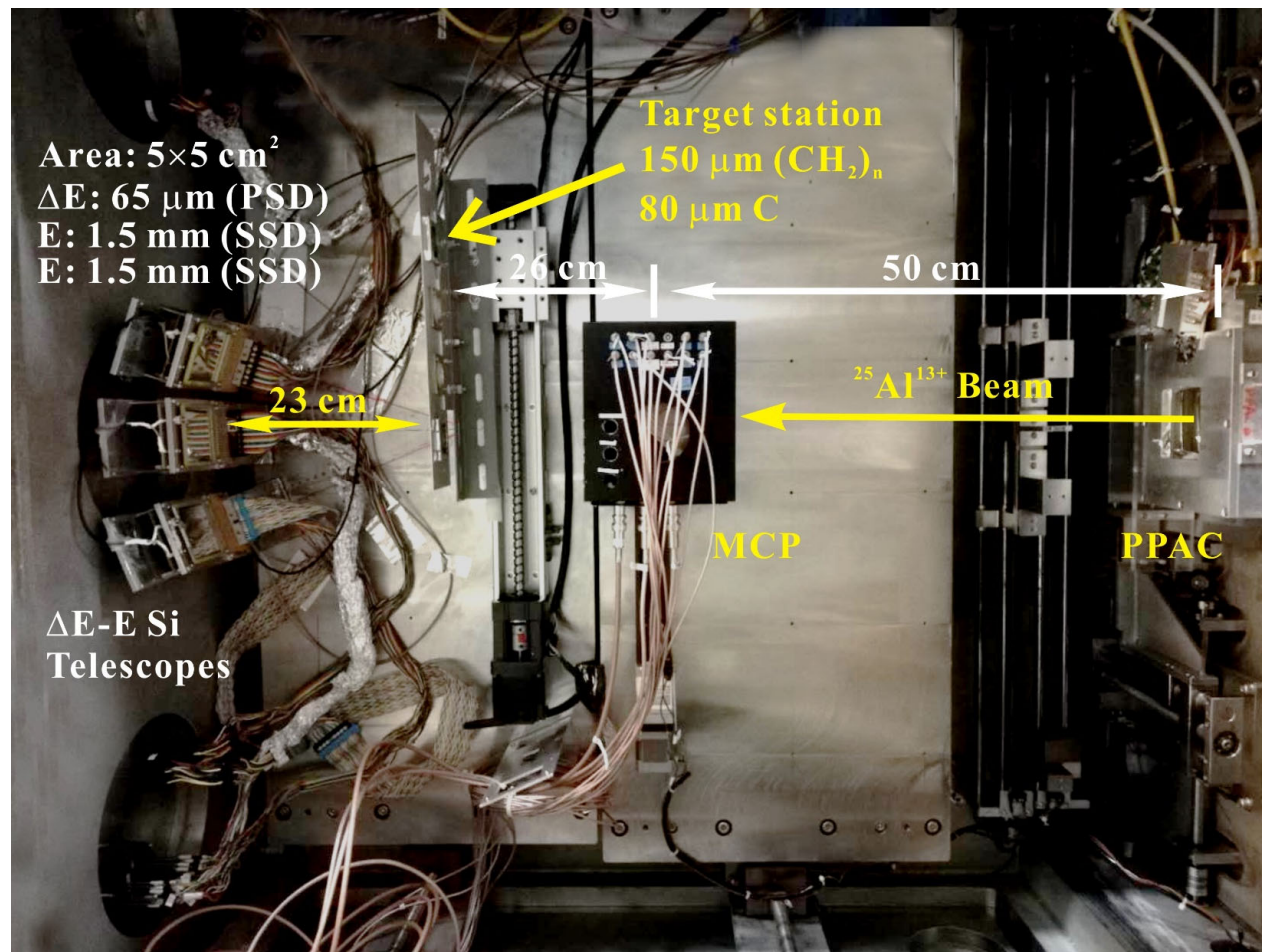
# Status of resonance studies



Experimental technique	$E_{\text{res}}$	$J^{\pi}$	$\Gamma_{p0}$	$\Gamma_{p'}$	$\Gamma_{\alpha}$
$\beta$ -delayed proton measurement of $^{26}\text{P}$ Thomas <i>et al.</i> 2004	$E_x > 10$ MeV	Shell model calculation	—	—	—
$^{28}\text{Si}(p,t)^{26}\text{Si}$ Matic <i>et al.</i> 2011	$E_x < 10$ MeV	Analog state assignment	—	—	—
$^{25}\text{Al} + p$ scattering measurement above the $\alpha$ threshold of $^{26}\text{Si}$ (present work)	Covering the relevant range, $E_x = 9-11$ MeV	R-Matrix fitting	$^{25}\text{Al}(p,p)^{25}\text{Al}$	$^{25}\text{Al}(p,p')^{25}\text{Al}$	—

**Experimental  
Setup at F3 focal  
plane**

**$^{25}\text{Al}$  beam:  
 $2 \times 10^5$  pps, 80%  
purity**

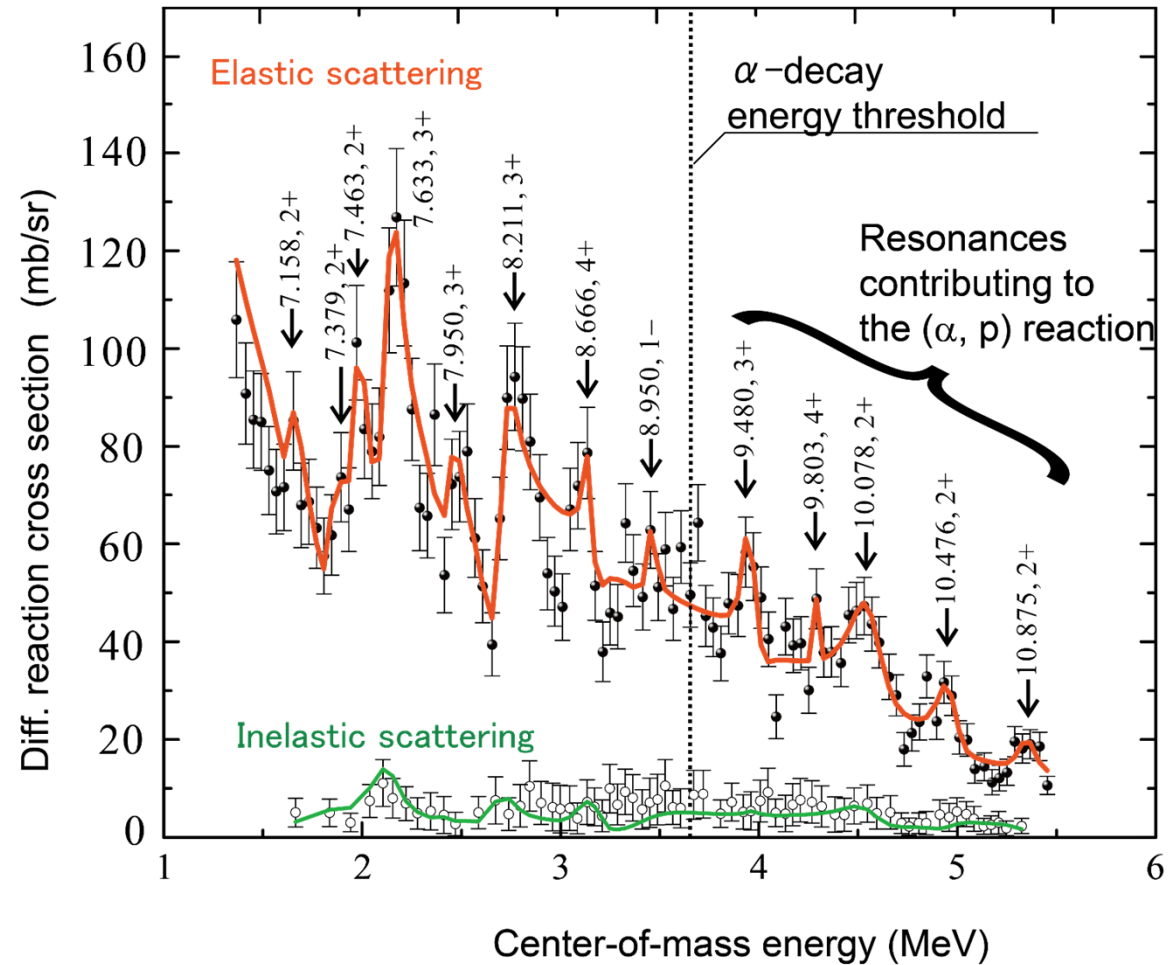


**$^{25}\text{Al}$  RI beam** at CRIB,  $(142 \pm 1)$  MeV,  
 $2 \times 10^5$  pps, 80% purity.

**Resonances** in  $^{26}\text{Si}$  are scanned by  
proton resonant scattering of  $^{25}\text{Al} + p$   
... exit channel of  $^{22}\text{Mg}(\alpha, p)$ .

The spin parities of 5 states above the  
 $\alpha$  threshold were determined for the  
first time ... reaction rate evaluated  
with parameters of those resonances  
( $E, J^\pi, \Gamma_p$ ).

$\Gamma_\alpha$  were not known from the  
measurement, and evaluated with the  
spectroscopic factor of the mirror  $^{26}\text{Al}$   
nucleus by Matic et al.



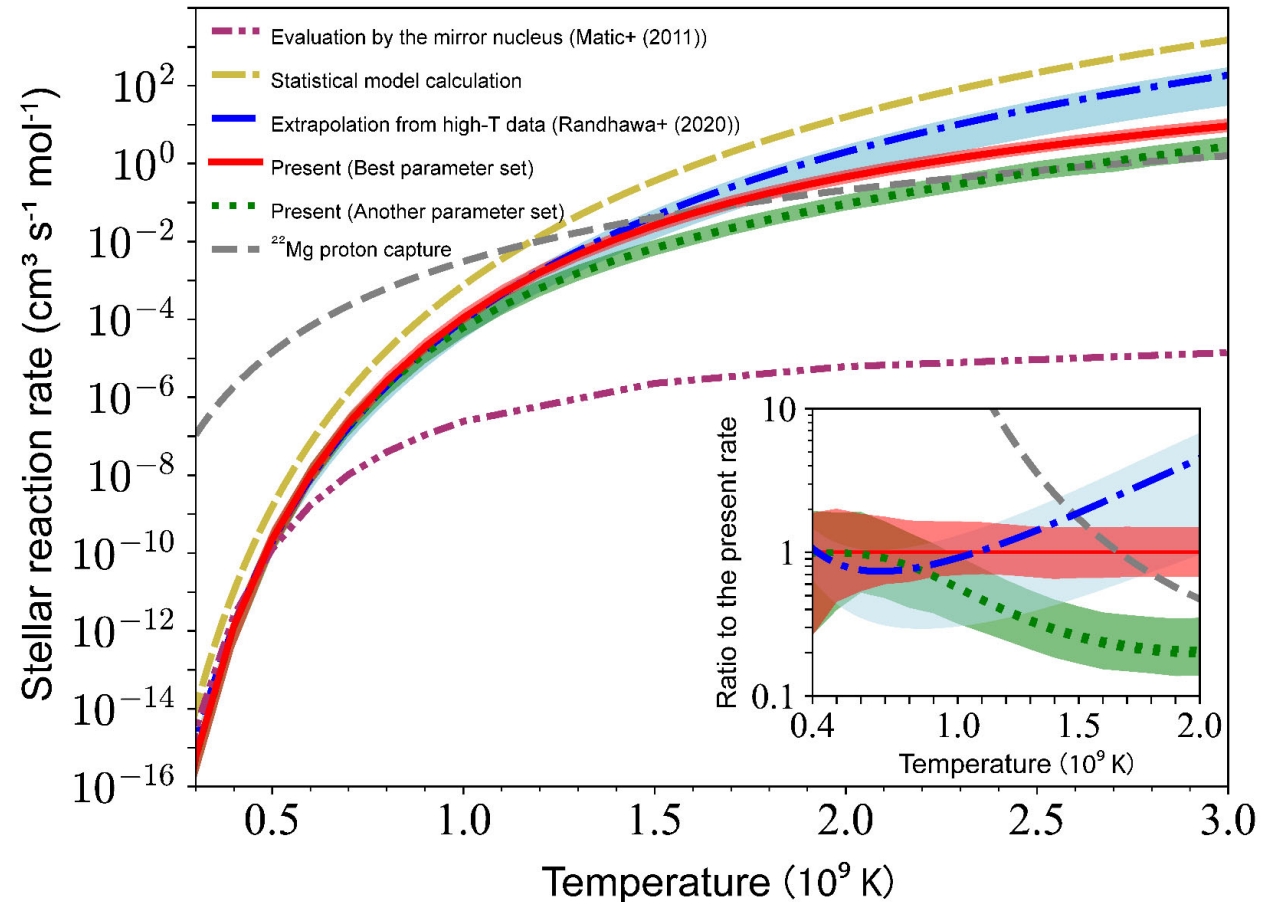
# Updated $^{22}\text{Mg}(\alpha,p)$ reaction rate

Red curve ...our new rate (resonant reaction rate)

Blue curve... MSU latest work (extrapolation)

These two are not too much different for the X-ray burst temperature.

Our uncertainty is mostly smaller than MSU, even though the error associated with extrapolation with statistical model calculation is not included in their evaluation.



# X-ray burst simulations

Light curves with a new XRB model (by Dr. Lam Yi Hua)

→ Improved reproducibility of the observational data (GS1826-24, SAXJ1808.4-3658).  $^{22}\text{Mg}(\alpha,p)$  produces a **visible effect**.

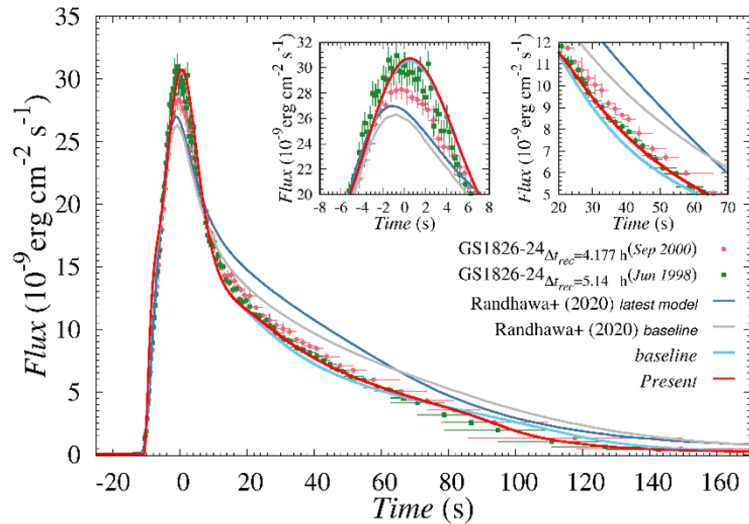


FIG. 3. The best fit *baseline* and *Present* modeled lightcurves to the observed lightcurve of epoch *Jun 1998*, and the best fit *Randhawa et al.* [22] lightcurves to epoch *Sep 2000*. The magnified lightcurves at the burst peak and  $t=20\text{--}70$  s are shown in the left and right insets, respectively.

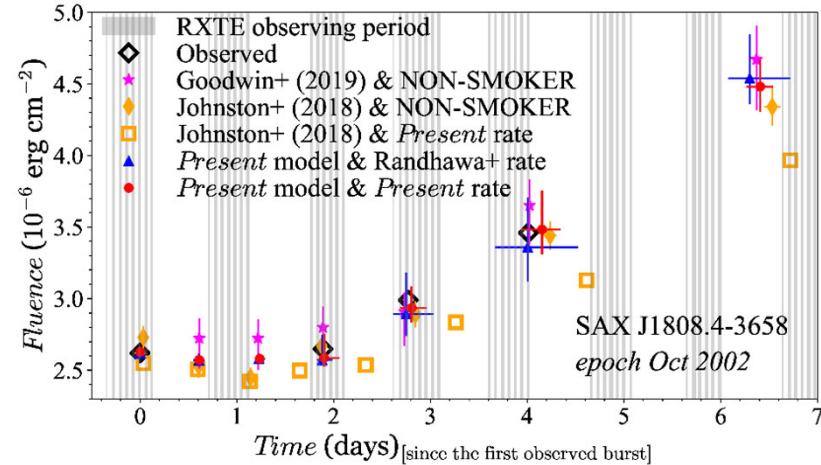
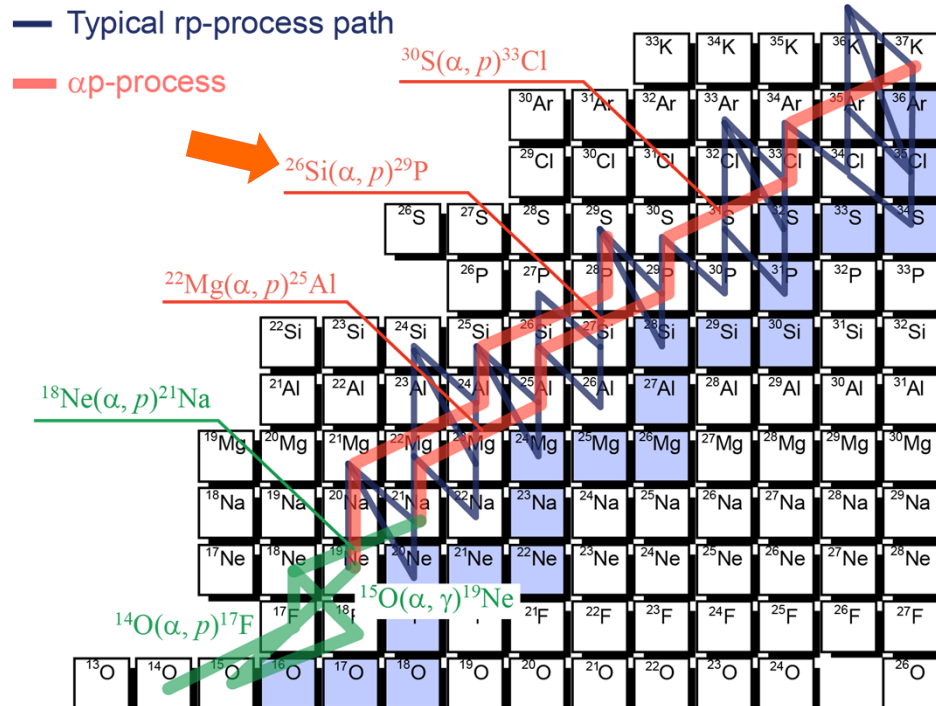


FIG. 4. The bursts' fluences (integration of flux over time) and times for SAX J1808.4-3658 burster, based on the RXTE observation [4], Johnston *et al.* [8] and Goodwin *et al.* [9] models, and present calculations. Johnston *et al.* [8] model is adopted to study the present and Randhawa *et al.* rates.

# The $^{26}\text{Si}(\alpha, p)^{29}\text{P}$ reaction



**Table 1**  
 Reactions that Impact the Burst Light Curve in the Single-zone X-Ray Burst Model

Rank	Reaction	Type <sup>a</sup>	Sensitivity <sup>b</sup>	Category
1	$^{56}\text{Ni}(\alpha, p)^{59}\text{Cu}$	U	12.5	1
2	$^{59}\text{Cu}(p, \gamma)^{60}\text{Zn}$	D	12.1	1
3	$^{15}\text{O}(\alpha, \gamma)^{19}\text{Ne}$	D	7.9	1
4	$^{30}\text{S}(\alpha, p)^{33}\text{Cl}$	U	7.8	1
5	$^{26}\text{Si}(\alpha, p)^{29}\text{P}$	U	5.3	1
6	$^{61}\text{Ga}(p, \gamma)^{62}\text{Ge}$	D	5.0	1
7	$^{23}\text{Al}(p, \gamma)^{24}\text{Si}$	U	4.8	1
8	$^{27}\text{P}(p, \gamma)^{28}\text{S}$	D	4.4	1

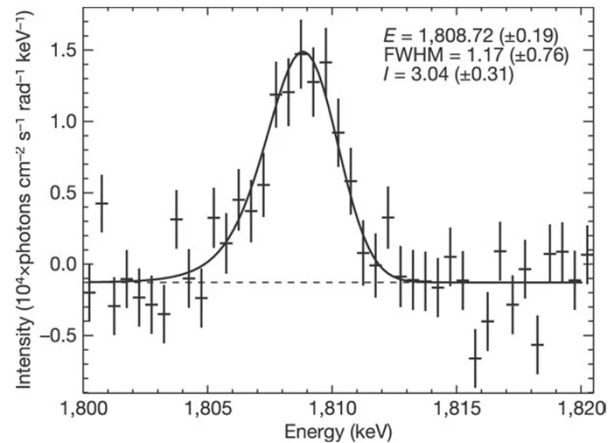
**Table 2**  
 Reactions that Impact the Burst Light Curve in the Multi-zone X-ray Burst Model

Rank	Reaction	Type <sup>a</sup>	Sensitivity <sup>b</sup>	Category
1	$^{15}\text{O}(\alpha, \gamma)^{19}\text{Ne}$	D	16	1
2	$^{56}\text{Ni}(\alpha, p)^{59}\text{Cu}$	U	6.4	1
3	$^{59}\text{Cu}(p, \gamma)^{60}\text{Zn}$	D	5.1	1
4	$^{61}\text{Ga}(p, \gamma)^{62}\text{Ge}$	D	3.7	1
5	$^{22}\text{Mg}(\alpha, p)^{25}\text{Al}$	D	2.3	1
6	$^{14}\text{O}(\alpha, p)^{17}\text{F}$	D	5.8	1
7	$^{23}\text{Al}(p, \gamma)^{24}\text{Si}$	D	4.6	1
8	$^{18}\text{Ne}(\alpha, p)^{21}\text{Na}$	U	1.8	1
9	$^{63}\text{Ga}(p, \gamma)^{64}\text{Ge}$	D	1.4	2
10	$^{19}\text{F}(p, \alpha)^{16}\text{O}$	U	1.3	2
11	$^{12}\text{C}(\alpha, \gamma)^{16}\text{O}$	U	2.1	2
12	$^{26}\text{Si}(\alpha, p)^{29}\text{P}$	U	1.8	2
13	$^{17}\text{F}(\alpha, p)^{20}\text{Ne}$	U	3.5	2
14	$^{24}\text{Mg}(\alpha, \gamma)^{28}\text{Si}$	U	1.2	2

•R.H. Cyburt *et al.*, *Astrophys. J.* **830**, 55 (2016).

- The  $^{26}\text{Si}(\alpha, p)^{29}\text{P}$  reaction has a high sensitivity on the light curve

# Effect on the $^{26}\text{Al}$ abundance



R. Diehl et al., Nature **439**, 45 (2006)

- The galactic 1.808 MeV gamma ray of  $^{26}\text{Al}$ 
  - ◆ Evidence of the ongoing process of the nucleosynthesis
  - ◆ Doppler shift of the line => rotation of the Galaxy
- The  $^{26}\text{Si}(\alpha, p)^{29}\text{P}$  reaction has also sensitivity on the abundance of  $^{26}\text{Al}$

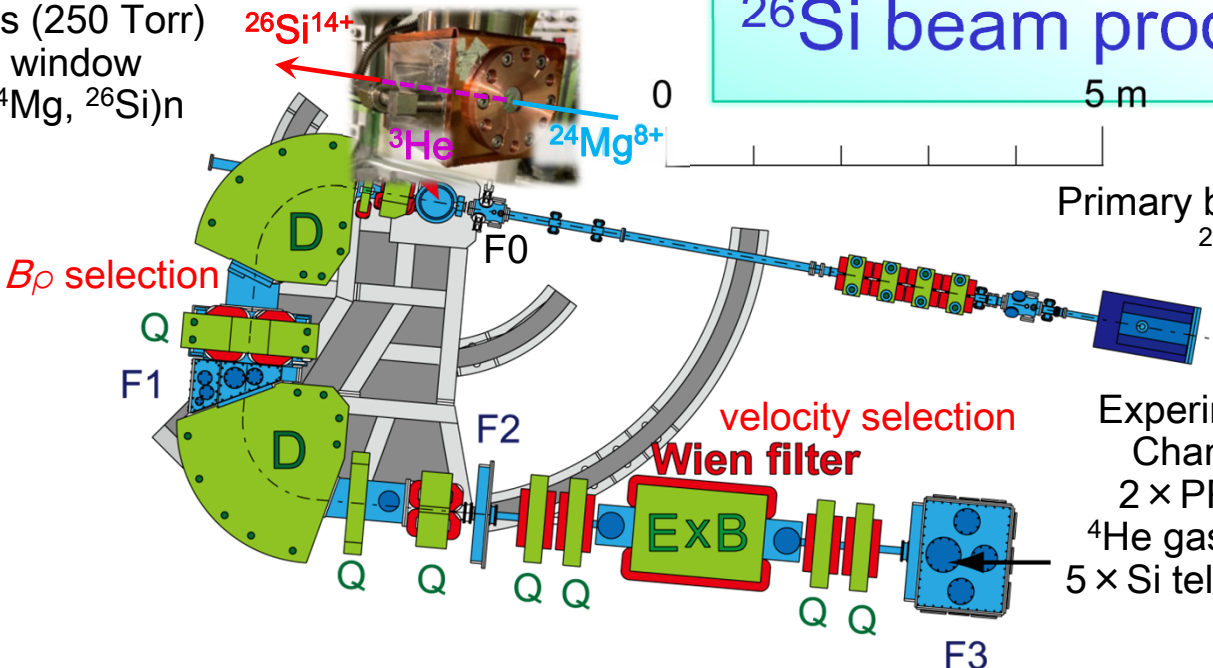
TABLE 3  
SAME AS TABLE 1, BUT FOR MODEL F08 (FISKER ET AL. 2008)

Reaction	Isotope	10	0.1
$^{12}\text{C}(p, \gamma)^{13}\text{N}$ .....	$^{12}\text{C}$	0.41	...
$^{12}\text{C}(\alpha, \gamma)^{16}\text{O}$ .....	$^{12}\text{C}$	0.42	...
	$^{16}\text{O}$	3.27	0.36
	$^{20}\text{Ne}$	3.03	0.42
	$^{24}\text{Mg}$	2.40	...
$^{16}\text{O}(\alpha, \gamma)^{20}\text{Ne}$ .....	$^{16}\text{O}$	0.11	8.36
$^{20}\text{Ne}(\alpha, \gamma)^{24}\text{Mg}$ .....	$^{20}\text{Ne}$	0.10	9.84
$^{22}\text{Mg}(\alpha, p)^{25}\text{Al}$ .....	$^{25}\text{Mg}$	...	8.81
	$^{27}\text{Al}$	...	2.23
$^{24}\text{Mg}(p, \gamma)^{25}\text{Al}$ .....	$^{25}\text{Mg}$	3.02	0.43
$^{24}\text{Mg}(\alpha, \gamma)^{28}\text{Si}$ .....	$^{24}\text{Mg}$	0.18	4.16
	$^{25}\text{Mg}$	0.24	4.10
$^{25}\text{Al}(\alpha, p)^{28}\text{Si}$ .....	$^{25}\text{Mg}$	0.22	2.36
$^{26g}\text{Al}(p, \gamma)^{27}\text{Si}$ .....	$^{27}\text{Al}$	2.71	0.40
$^{26g}\text{Al}(\alpha, p)^{29}\text{Si}$ .....	$^{26g}\text{Al}$	...	2.34
	$^{26g}\text{Al}$	0.08	2.38
	$^{27}\text{Al}$	0.40	...
$^{26}\text{Si}(\alpha, p)^{29}\text{P}$ .....	$^{26g}\text{Al}$	0.08	...
	$^{27}\text{Al}$	0.23	...
$^{27}\text{Al}(\alpha, p)^{30}\text{Si}$ .....	$^{27}\text{Al}$	0.32	...
$^{27}\text{Si}(\alpha, p)^{30}\text{P}$ .....	$^{27}\text{Al}$	0.30	...
$^{28}\text{Si}(\alpha, \gamma)^{32}\text{S}$ .....	$^{28}\text{Si}$	0.43	...
	$^{32}\text{S}$	3.73	0.37

Parikh et al., Astrophys. J. Suppl. Ser. **178**, 110 (2008)

# $^{26}\text{Si}$ beam production at CRIB

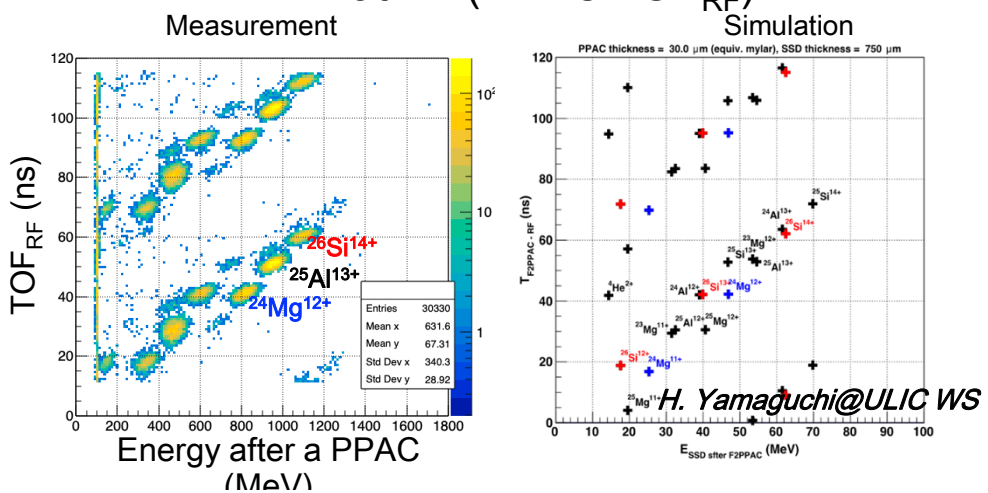
LN<sub>2</sub>-cooled gas target  
 $^3\text{He}$  gas (250 Torr)  
 Mo window  
 $^3\text{He}(^{24}\text{Mg}, ^{26}\text{Si})\text{n}$



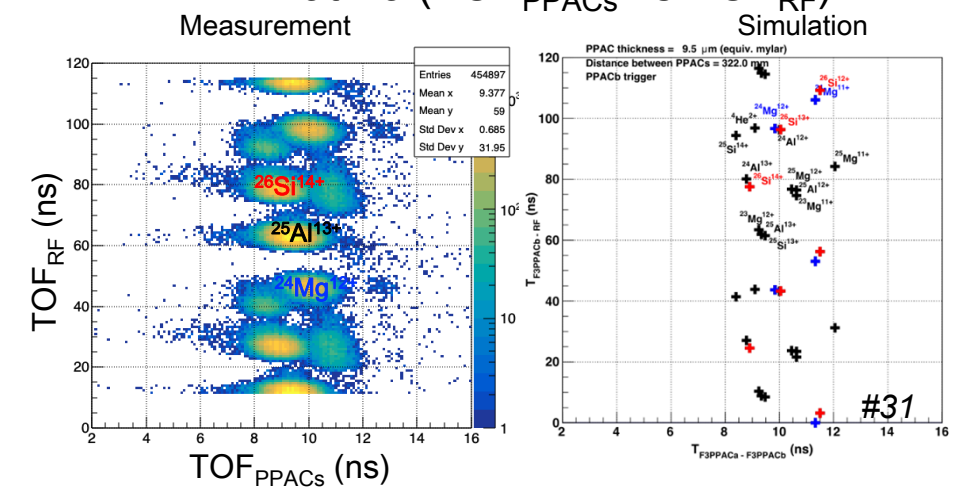
Primary beam from AVF cyclotron  
 $^{24}\text{Mg}$ , 7.55 MeV/u

Experimental Chamber  $^{26}\text{Si}^{14+}$  beam ~ 29%,  
 2 × PPACs 4.5 MeV/u,  $3 \times 10^4$  pps on target  
 $^4\text{He}$  gas target  
 5 × Si telescopes

PID at F2 ( $\Delta E$  vs  $\text{TOF}_{\text{RF}}$ )



PID at F3 ( $\text{TOF}_{\text{PPACs}}$  vs  $\text{TOF}_{\text{RF}}$ )



# Thick target in inverse kinematics + $^{26}\text{Si}$ beam

TTIK scan,  $E_{\text{c.m.}}$  up to 7.3 MeV

$\alpha$  resonant scattering measurement

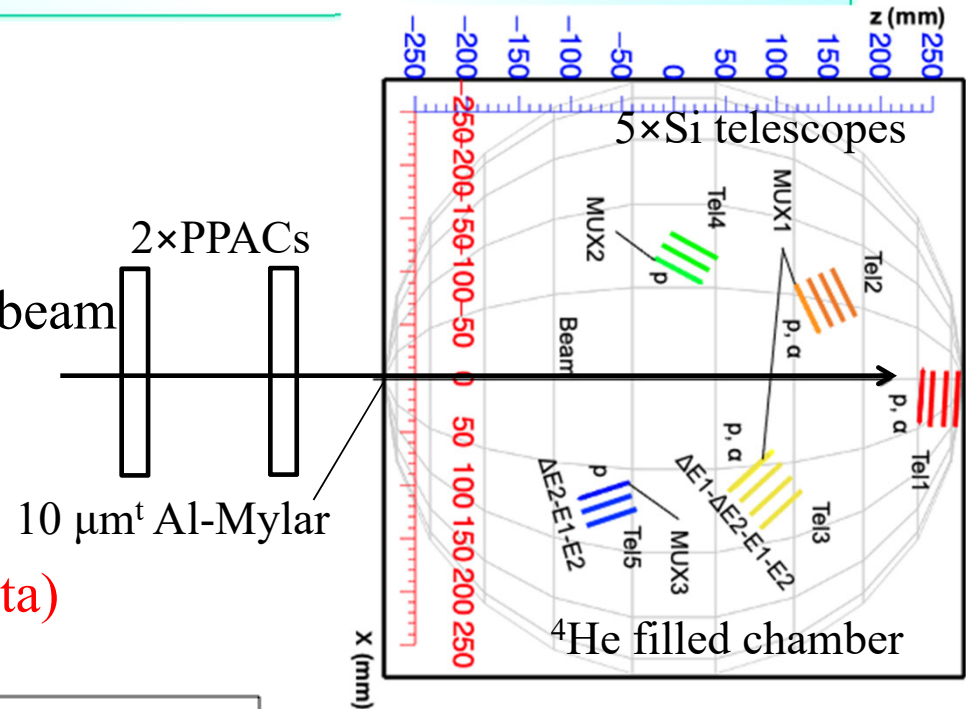
$\alpha$  resonances,  $\alpha$  clustering structure

R-matrix analysis  $\rightarrow$  to determine  $\Gamma_{\alpha}$

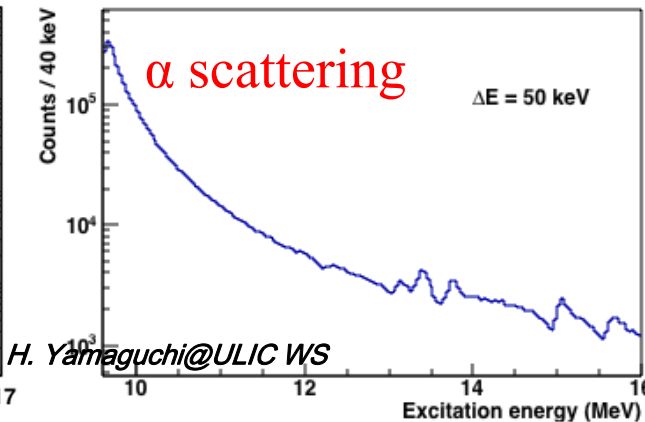
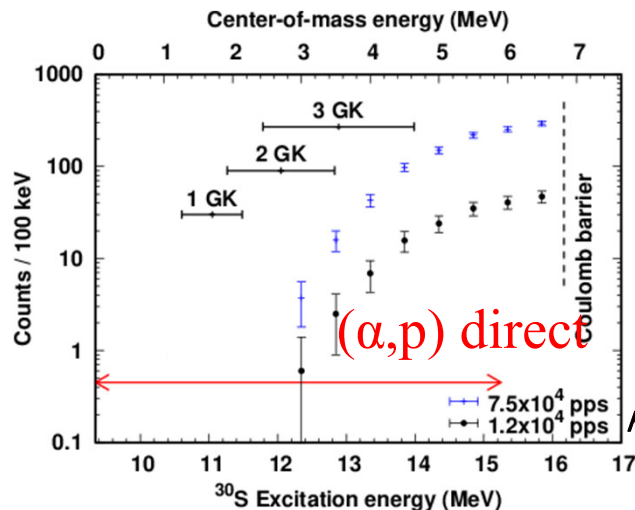
( $\ll \Gamma_p$ , dominant in  $\langle \sigma_R \rangle \propto \Gamma_{\alpha} \Gamma_p / \Gamma_{\text{tot}} \sim \Gamma_{\alpha}$ )

$(\alpha, p)$  reaction direct measurement

Reasonable statistics down to  $E_{\text{c.m.}} \sim 3$  MeV

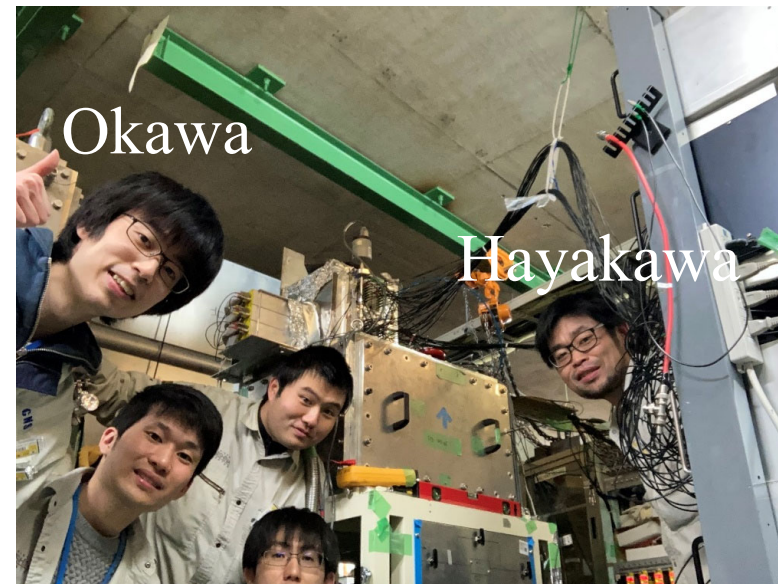


Yield estimation (not actual data)



# Collaboration/ beamtime

**CNS:** S. Hayakawa, K. Okawa, N.R. Ma, H. Shimizu H. Yamaguchi, Q. Zhang,  
T. Chillery, S. Hanai, N. Imai, J. Li, S. Michimasa, R. Yokoyama  
**SKKU:** K.Y. Chae, M.J. Kim, N.N. Duy, G.M. Gu, C.H. Kim, S.H. Kim, M.S. Kwag,  
N.K. Uyen,  
**IBS:** S.M. Cha, D. Kim  
**Osaka:** S. Adachi, T. Furuno, K. Sakanashi, T. Kawabata  
**ELI-NP:** D. Kahl, O. Sirbu  
**RIKEN:** S. Kubono



The first CRIB main experiment after COVID.

Foreign collaborators could not come to Japan from due to COVID19 restriction

Domestic collaborators from Osaka U. and CNS

Online communication during the machine time (Zoom + Slack + YouTube live)

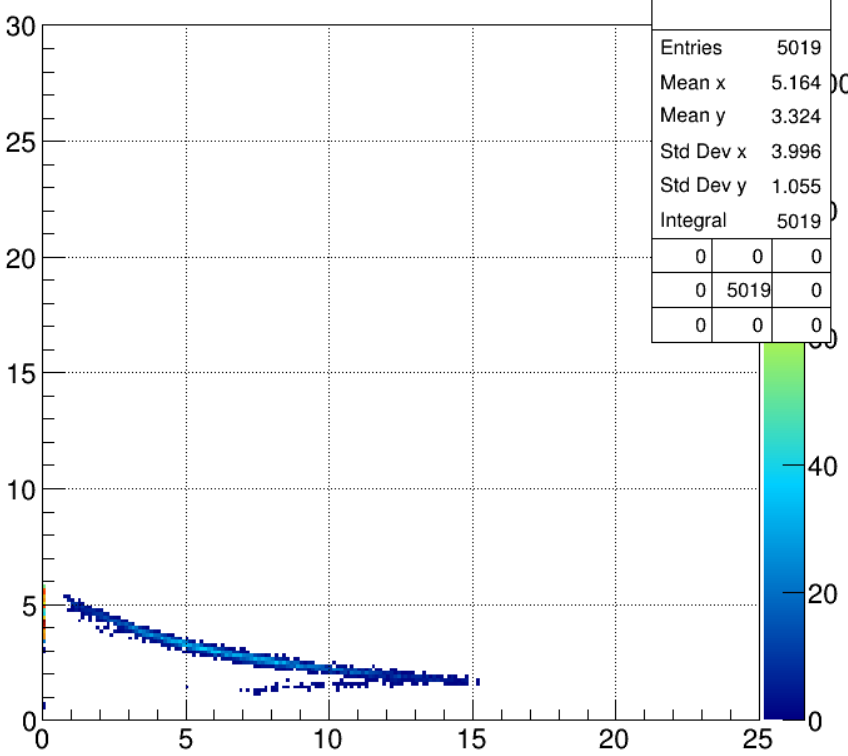
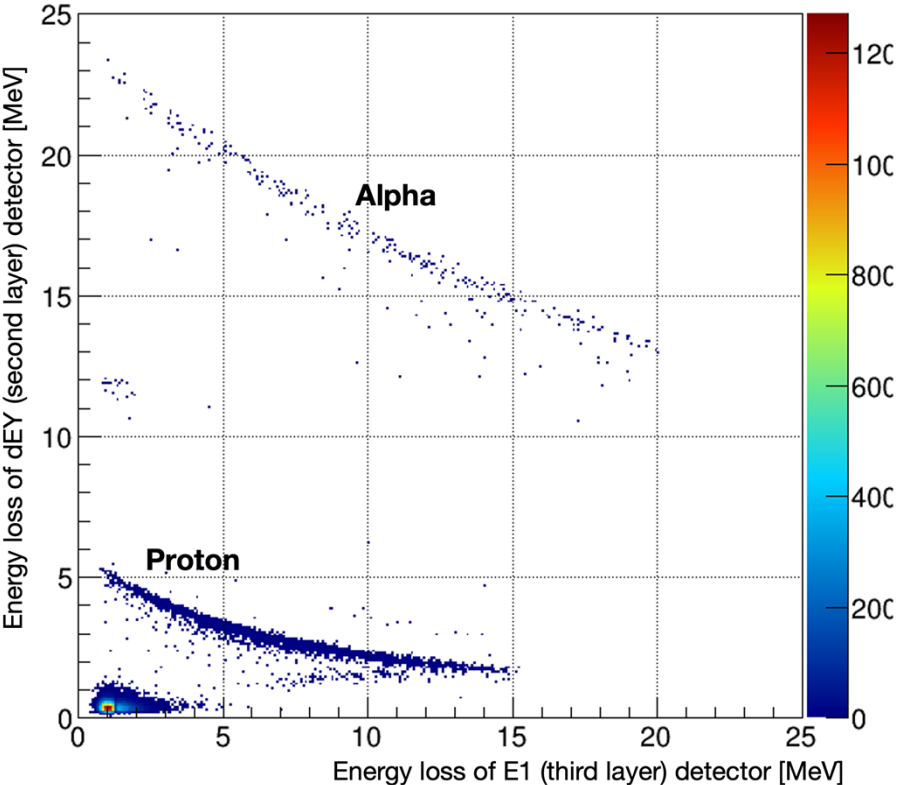
Graduate students working on analysis (Okawa, M.J. Kim)



H. Yamaguchi@ULIC WS

# Proton event selection

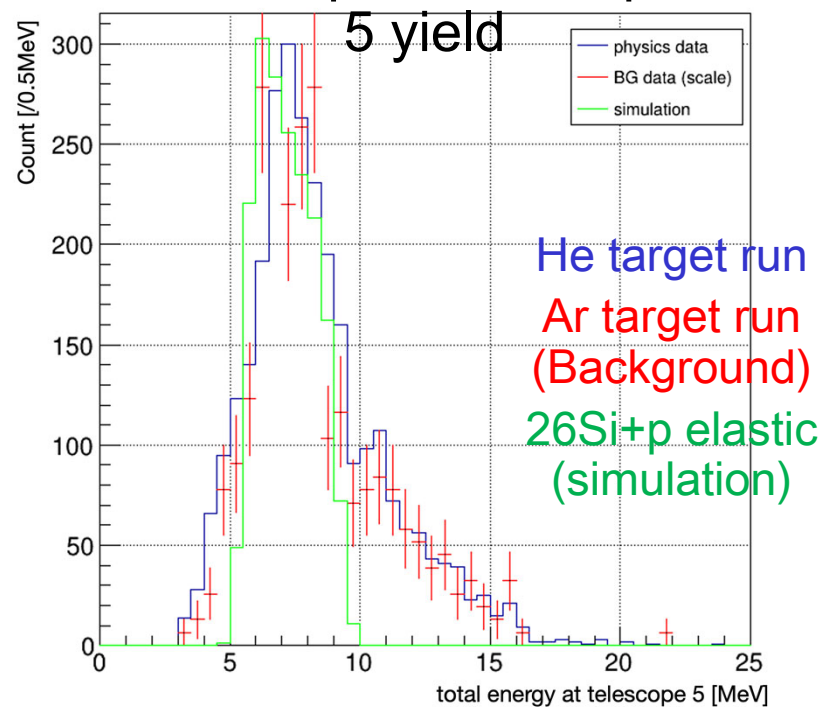
$\alpha$  and  $p$  were clearly identified. Selected proton events as candidates of  $(\alpha, p)$  reaction products



# Background from the elastic scattering of $^{26}\text{Si} + p$

- Low energy (<10 MeV) proton events were likely to be elastic scattering at the window (Mylar  $\text{C}_{10}\text{H}_8\text{O}_4$ ) → consistent with a Monte Carlo calculation

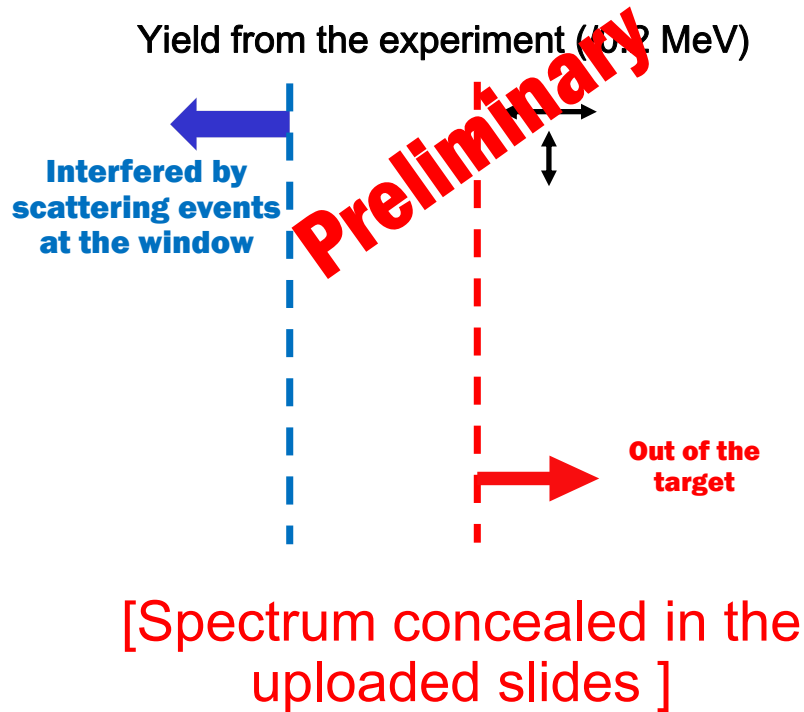
## •Example: Telescope



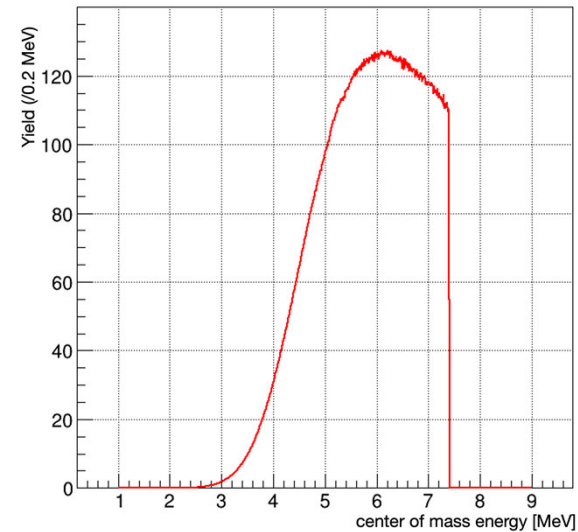
- However, spectra of the He-target run and Ar-target background run are still similar in 10 – 15 MeV region.

Evaluated the yield of the  $(\alpha,p)$  reaction by subtracting all proton events from the background events

# Yield compared with calculation



Simulation with NON-SMOKER cross section



- The subtracted yield was **lower than theoretical yield by over one order of magnitude**
  - Experiment: ~ 5 events vs calculation: ~ 120 events, per 0.2 MeV, around 7.0 MeV

# Summary

- CRIB is an RI beam facility in RIBF operated by CNS, the University of Tokyo, providing low-energy (<10MeV/u) in-flight RI beams with high intensity and purity.
- Unique studies with low-energy RI beams have been made. Recent highlights are:
  - $^{22}\text{Mg}(\alpha, p)$  reaction study with the resonant scattering method  
→ Reaction rate updated with the resonant reaction evaluation. Implication to the X-ray burst light curve was discussed.
  - $^{26}\text{Si}(\alpha, p)$  reaction study with the direct measurement.  
→ The preliminary result shows the yield seems to be more than factor 10 lower than the theoretical calculation.
- We welcome new collaborators and new ideas. Please contact with me if you have any idea.
- Visit CRIB webpage for more information. <http://www.cns.s.u-tokyo.ac.jp/crib/crib-new/>